Exp. Theo. NANOTECHNOLOGY 10 (2026) 571-584 https://doi.org/10.56053/10.2.571

Evaluation of influence of different parameters on positron radiation emitter ^{18}F- Fuorodeoxyglucose uptake for positron emission tomography/computed tomography scans in tumors and healthy organs

Marwa Safa Riyadh[*], *Samar I. Essa*

Department of Physics, College of Science, University of Baghdad, Baghdad, Iraq
[*]) Email: samar.o@sc.uobaghdad.edu.iq

Received 8/2/2026, *Received in revised form* 8/3/2026, *Accepted* 19/3/2026, *Published* 15/4/2026

Background: In nuclear medicine diagnostics, nanomaterials are being utilized more and more to enhance radiotracer performance and targeting in imaging modalities including Positron Emission Tomography and Single Photon Emission Computed Tomography. They improve picture quality, sensitivity, and specificity for early illness diagnosis due to their small size and capacity to transport radioactive isotopes. Clinical practice frequently uses Positron Emission Tomography/Computerized Tomography (PET/CT) as a routine procedure for imaging cancer and other disorders. Even though there are other radiotracers available, 18F-FDG is the most often used one. Protocols for patients' appropriate preparation prior to 18F-FDG injection are recommended by international PET/CT guidelines, specifically for patients with diabetes. Objective: This study aims to investigate the influence of various factors on the maximum SUV measurements in normal and tumor organs, such as body weight and body mass index. Methods: A total of 300 patients, consisting of 173 females, 127 males, aged between 18 and 88 years., are selected retrospectively. Every patient had undergone 18F-FDG utilizing the established imaging technique. Before undergoing PET-CT imaging, all patients abstained from eating for a minimum of 6 hours, and their blood glucose levels (BGL) while fasting are within the normal range. Following the intravenous infusion of 18F-FDG The whole-body PET/CT scan is performed approximately 45-90 minutes after the injection of 18F-FDG, and images are taken from the top of the head to the upper thigh area. The factors examined included the administered dose of 18FFDG (in mCi), age (in years), BGL (in mg/dl), height (H) (in cm), and weight (W)(in kg). The BMI is computed and the SUV max is determined based on the BMI and 18F-FDG. Results: After conducting the necessary statistical calculations, the results indicated a substantial rise in SUV values among individuals who are obese. BMI is the most effective independent variable in predicting the SUV value. Conclusions: Understanding the natural absorption of 18F-FDG and the standard uptake

values (SUVs) of normal and tumor organs is necessary to accurately interpret whole-body 18F-FDG-PET/ CT studies.

Keywords: Normal Organs; PET/CT; ^{18}F-FDG; Body mass index.

1. INTRODUCTION

In hybrid imaging systems like PET/CT scanners, nanomaterials have emerged as a crucial link between nanotechnology and nuclear medicine [1-5]. They can serve as sophisticated carriers for radiotracers used in positron emission tomography because of their special physicochemical characteristics, which include large surface area, tunable surface chemistry, and nanoscale size. Nanoparticles can be designed to deliver radioactive isotopes to particular tissues or tumors in a selective manner for PET imaging [6-10]. This tailored distribution reduces radiation exposure to healthy tissues while increasing diagnostic sensitivity and image contrast [1]. Additionally, radiotracer stability in the bloodstream is improved, circulation time is extended, and molecular-level imaging of disease processes is made possible by functionalized nanomaterials. Nanomaterials can function as dual-modality contrast agents when paired with CT, offering High-Z elements for CT attenuation enhancement and radioactive tagging for PET. More precise quantitative analysis and anatomical localization are supported by this combination. Furthermore, radioactive nanoparticles can simultaneously detect and treat cancer thanks to theranostics, a combination therapeutic and diagnostic technique made possible by nanotechnology [11-15]. All things considered, the combination of nanomaterials and PET/CT technology is a significant development in nuclear medicine that enhances focused radiation, tailored diagnostics, and precision imaging while lowering systemic toxicity [2]. Currently, positron emission tomography (PET) with integrated computed tomography (CT) imaging is the most advanced method for functional imaging [16-20]. 18F-fluorodeoxyglucose (18F-FDG) can serve as an imaging agent by exploiting the increased glucose metabolism in cancerous tumors [3]. As the most widely used radiopharmaceutical for PET studies of cancer, 18F-FDG PET/CT can evaluate basic changes in the cellular metabolism of glucose that are common to all neoplasms. However, to accurately interpret 18F-FDG-PET pictures, it is necessary to understand the physiological distribution of the tracer molecule in normal organs, as well as their standardized uptake value (SUV) [4]. It follows that the SUV must be used for a semiquantitative study of the PET data. The SUV is a widely used tool for measuring the static accumulation of FDG in tissues [21-25]. Often called a semi-quantitative metric, the SUV is not a real kinetic rate constant [5]. In this work, we applied the most widely used SUV computation, which is as follows [6, 26-30]:

$$\mathrm{SUV(g/ml)} = \frac{\text{average activity in ROI (MBq/ml)}}{\text{injected dose (MBq)}} \times \text{bodyweight (g)} \qquad (1)$$

Several factors, including body mass index (BMI), sex, length of uptake time, and given 18F-FDG dosage, can influence the accuracy of SUV assessment. Also, there isn't a consensus on how glycemia actually affects 18F-FDG absorption because different studies [7–9] have found different effects of blood glucose on SUVs in different organs. Both American [10] and European [11] guidelines recommend testing blood glucose before PET/CT scanning, and postponing the examination if the result exceeds 200 mg/dl. Rescheduling of this kind, nevertheless, can be inconvenient for both patients and nuclear medicine practices. It's critical to understand that physiological 18F-FDG buildup can occasionally resemble disease and can be substantial in particular organs [12]. Understanding this physiological activity is critical for accurately interpreting whole-body 18F-FDG-PET studies. SUV is useful not only for studying glucose metabolism, but also for measuring radiopharmaceuticals like thymidine and choline [31-35]. Understanding the physiological uptake of 18F-FDG and the variability

of normal organ SUVs is necessary for the proper interpretation of 18F-FDG-PET imaging [13]. This study examined the SUVs of normal and tumor organs (liver, bone, and lung) [36-40].

2. PATIENTS AND METHODS

2.1. Patient population

The study included 300 participants (173 females, 127 males), mean age 58.95±15.38). Aged between 18 and 88 years, body weights ranged from 37 to 130 kg, with a mean weight of 73.58± 16.15, referred to AL- Safeer Specialist Hospital / Baghdad during March 2024 until Jun 2024. This study does not require ethical approval. We instructed patients to fast for at least four to six hours before receiving FDG. We instructed them not to perform any heavy muscular activity 24 hours before the exam to prevent unnecessary uptake and minimize the imaging background. We advised them to consume 1 liter of water within two hours prior to the FDG administration, to ascertain whether the concentration is within the standard range (<120 mg/dl for non-diabetic individuals and 150–200 mg/dl for diabetics), blood glucose levels are also tested. Rescheduling is taken into consideration if the serum glucose levels are higher than the typical range [41-45]. We obtained a complete patient history, which included information on previous treatment with chemotherapy, radiation, or any other experimental therapeutics. We reported the 18F-FDG injection dose (mCi), the patients' age (years), glycemia at the time of the trial (mg/dl), as well as their height (cm) and weight (kg). We then computed the BMI using the following formula [14]:

$$BMI = \frac{weight\ in\ kg}{(height\ in\ m)^2} \tag{2}$$

Table 1 Classification of national status based on BMI [14].

Body mass index (BMI)	Category
Less than or equal to 18.4 Low weigh	Low weight
18.5 to 24.9	Normal weight
25 to 29.9	Overweight
30 to 34.9	Obese grade I
35 to 39.9	Obese grade II
Greater than or equal to 40	Obese grade III

The body mass index (BMI) is classified by the World Health Organization as follows: underweight (BMI < 18.5 kg/m^2), normal (BMI between 18.5 and 24.99 kg/m^2), overweight (BMI between 25 and 29.9 kg/m^2), and obese (BMI < 30 kg/m^2), Table 1 [14]. We optimized the waiting settings, preparation area, and room temperature to ensure optimal resting conditions during and after FDG administration, thereby minimizing muscle and brown-fat uptake. We instructed patients to void their bladders before entering the PET examination room. We positioned the patients in a supine position, raising their arms and placing their heads first [46-50]. The procedure began with a CT scan for attenuation correction, followed by the movement of the bed shuttle to initiate the PET phase of the treatment [51-55]. During

the PET/CT session, we advised patients to maintain stillness and practice shallow breathing. We kept artifacts, metals, and other attenuation-causing objects at a distance to preserve image quality and prevent attenuation [56-58]. We collected emission data between 45 and 90 minutes after the delivery of 18F-FDG. We input the decay times and accurate isotopes into the acquisition computer. To provide precise measurements, the dosage calibrator is cross-calibrated with the scanner time [60-65].

2.2. PET/CT examinations

We used the 'big-bore' technology that Philips introduced. The detector of this scanner consisted of crystals constructed from lutetium-yttrium oxyorthosilicate (LYSO), with dimensions of (4 × 4 × 22) millimeters. A CT facility equipped with a 64-slice scanner is utilized, employing a consistent tube voltage of either 90, 120, or 140 kilovolts peak (kVp). The tube current time product (mAs) varied between 20 and 500 mAs. The patients are positioned in a supine position with both arms elevated. A dose of FDG at a concentration of 0.1 mCi per kilogram of body weight is given by an intravenous route. Immediately after, the PET scan is performed, followed by a diagnostic CT scan. Typically, it encompassed the area from the middle of the cranium to the upper part of the thigh. Images are acquired 45-90 minutes' post-injection of FDG. A low-dose CT scan is conducted to adjust for attenuation and scatter. The diagnostic CT exams are conducted using a tube voltage of 120 kV, and a rotation speed of 0.44 seconds. During normal tidal respiration, 3D PET acquisition is conducted at each bed position for 1-4 minutes. All data are corrected for dead time and random coincidences, in addition to attenuation and scatter correction [66-70].

2.3. Statistical analysis

Every result is expressed using the mean and standard deviation (SD). All statistical investigation is done using Microsoft Office Excel 2016. Using a paired and unpaired Student's t-test allowed one to compare data between variables. If $P < 0.05$ the outcome is regarded as statistically significant [71-73].

3. RESULTS AND DISCUSSIONS

Baseline characteristics of the normal study population are summarized in Table 2. The mean value of blood glucose is 108.9 ± 26.56, and the mean of BMI is 26.40±6.26. The average injected dose and injected dose/weight, mci/kg, are (7.13±1.15mCi), (0.10±0.10) mCi/kg, respectively.

Table 2 Characteristics of normal cases included in the study.

Parameters	Normal cases (n=150) Mean ±SD
Age, years	57.56 ± 15.87
Body mass, kg	69.50 ± 14.36
Height, m	1.62 ± 0.08
BMI, Kg/m^2	26.40 ± 6.26
^{18}F-FDG, mCi	7.13 ± 1.15
Blood glucose mg/dl	110.89 ± 29.42
Dose injected /weight, mci/kg	0.10 ± 0.10

After filling in all the values in the Table 2 about mean, deviation, injection dose (mCi), weight (W) (in kg), height (H) (in m), and BMI Kg/m^2 is calculated according to the formula 1. Subjects are classified into three categories based on their BMI values: normal, overweight, and obese, for bone. Table 3 shows that the values of BMI and injection dose for the normal weight group are (21.78±1.75)

and (6.52±0.33), respectively, with a p value < 0.05. Overweight group is (27.08±1.27) and (7.02 ±0.67), respectively, which is also significant. For the obese group, the mean values for both BMI and injection dose are (mean BMI 35.82±6.14, and injection dose 8.68±0.49, with p value < 0.05). For liver, BMI (kg/m^2) and injection dose for normal weight group is (mean BMI 22.09±1.73, and injection dose ,6.57±0.42, p value < 0.05). The value of BMI and injection dose for overweight group is (26.85±1.48) and (6.92±0.81), respectively with also significant. For obese group the mean values for both BMI and injection dose are (mean BMI 34.31±5.20, and injection dose 8.43±0.74, with p value < 0.05). Table 3 displays the average maximum 18F-FDG uptake of the tested lung for the three BMI groups. The higher 18F-FDG uptake increases with increasing BMI. We then obtained comparisons between the three groups, revealing a statistically significant difference between all groups. The relationships between the injection dose and BMI groups are shown in Figure 1. The Figures clearly show that injection dose increase with a BMI increase [74-76].

Table 3 Results for administered 18F-FDG.

Groups	Mean ± SD					
	W (kg)	H (m)	BMI $kg/(m)^2$	Injection dose (mCi)	Dose/weight (mci/kg)	p-value
For bone						
Normal weight	60.96±7.26	1.67±0.08	21.78±1.75	6.52±0.33	0.10±0.01	<0.05
Overweight	69.3±9.22	1.59±0.09	27.08±1.27	7.02 ±0.67	0.11±0.01	<0.05
Obese	90±12.12	1.58±0.05	35.82±6.14	8.68±0.49	0.09±0.01	<0.05
For liver						
Normal weight	61.5±7.22	1.66±0.07	22.09±1.73	6.57±0.42	0.10±0.01	<0.05
Overweight	66.2±11.80	1.54±0.11	26.85±1.48	6.92±0.81	0.11±0.01	<0.05
Obese	83.86±9.04	1.58±0.05	34.31±5.20	8.43±0.74	0.10±0.004	<0.05
For lung						
Normal weight	60.86±7.41	1.66 ±0.07	21.82±1.94	6.09±0.30	0.10±0.009	<0.05
Overweight	70.11±11.32	1.59±0.11	27.40±1.69	7.03±0.78	0.10±0.007	<0.05
Obese	88.91±11.84	1.57±0.06	35.83±5.46	8.96±0.90	0.10±0.005	<0.05

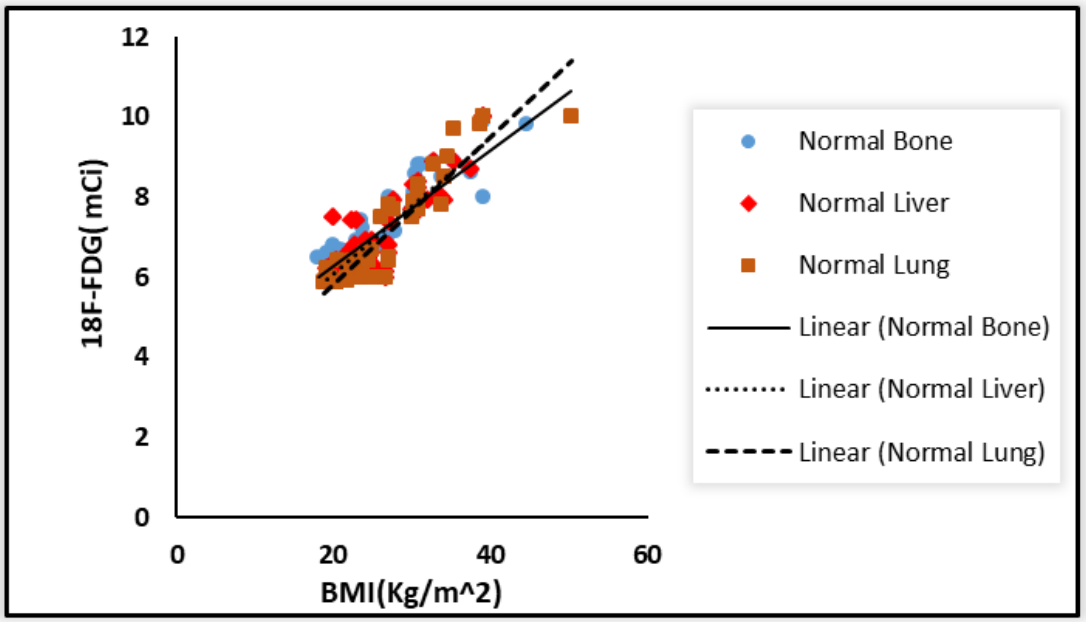

Figure 1 Relation between BMI and injection dose for normal tissue.

3.1. Relation between SUVmax with BMI

For bone, the mean value for SUVmax is (2.37 ± 0.30) and statistically significant with BMI for normal weight ($p < 0.05$), as shown in Table 4. The mean values for SUVmax for overweight and obese are (2.41 ± 0.26) and (2.53 ± 0.20), respectively, with also significant ($p < 0.05$). Upon examining the average liver SUV values based on BMI, Table 4, we observed a significant increase in SUV among obese individuals [77-80]. The mean value of BMI SUVmax is (2.40±0.07), (2.47±0.11), (2.72±0.10), for normal weight, overweight, and obese, respectively, the results showed a significant change between SUVmax and BMI, p value < 0.05. for liver Mean ± SD SUVmax, of the lung is shown in Table 4. Mean SUVmax in the lung is significantly higher in obese than those in normal BMI. The relationships between the injection dose and BMI and SUVmax are shown in Figure 2.

Table 4 SUVmax values based on BMI.

Groups	Mean ± SD				
	Weight (kg)	Height (m)	BMI kg/(m)^2	SUV_{max}(g/ml)	p-value
For bone					
Normal weight	60.96±7.26	1.67±0.08	21.78±1.75	2.37 ± 0.30	<0.05
Overweight	69.3±9.22	1.59±0.09	27.08±1.27	2.41 ± 0.26	<0.05
Obese	90±12.12	1.58±0.05	35.82±6.14	2.53 ± 0.20	<0.05
For liver					
Normal weight	61.5±7.22	1.66±0.07	22.09±1.73	2.40±0.07	<0.05
Overweight	66.2±11.80	1.54±0.11	26.85±1.48	2.47±0.11	<0.05
Obese	83.86±9.04	1.58±0.05	34.31±5.20	2.72±0.10	<0.05
For lung					
Normal weight	60.86±7.41	1.66 ±0.07	21.82±1.94	0.48 ± 0.07	<0.05
Overweight	70.11±11.32	1.59±0.11	27.40±1.69	0.53 ± 0.06	<0.05
Obese	88.91±11.84	1.57±0.06	35.83±5.46	0.63 ± 0.05	<0.05

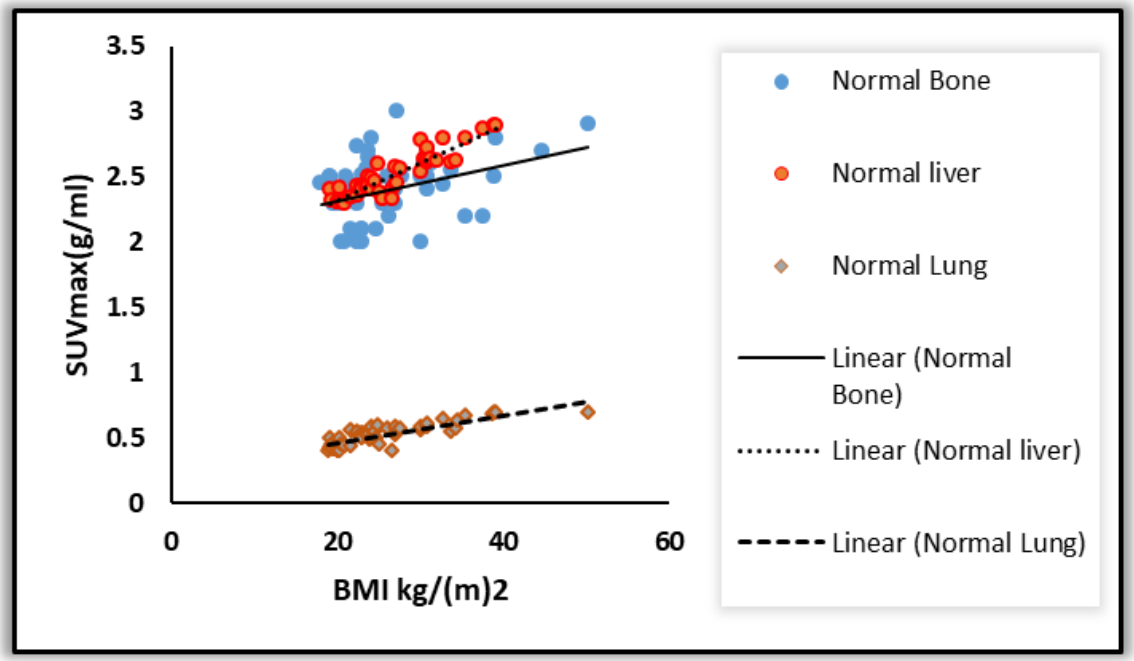

Figure 2 Relation between BMI and SUVmax for normal tissue.

3.2. Relation between injection dose with BMI for tumor

The data analysis of 150 patients, with 78 females and 72 males; a mean age of 60.50 ± 14.74 years, who underwent 18F-FDG PET examinations with a mean of 7.79 ± 1.35mCi). Mean ± SD dose injected/weight are (0.10 ± 0.02 mci/kg). Average body weight (77.50 ± 16.85kg) and height (1.65 ± 0.12 m). The blood glucose level is measured in all patients before injection. The average glucose level is (104.23 ± 20.55 mg/dl). The demographic data of patients are shown in Table 5.

Table 5 Characteristics of tumor included in the study.

Parameters	Tumor cases (n=150) Mean ±SD
Age, years	60.50 ± 14.74
Body mass, kg	77.50 ± 16.85
Height, m	1.65 ± 0.12
BMI, Kg/m^2	28.44 ± 6.31
^{18}F-FDG, mCi	7.79 ± 1.35
Blood glucose mg/dl	104.23 ± 20.55
Dose injected /weight, mci/kg	0.10 ± 0.02

Table 6 displays the average maximal 18F-FDG uptake of the tested tissues for the three BMI groups. The statistically significant effect is an increase in 18F-FDG uptake as BMI increased. The study evaluated the 18F-FDG PET/CT whole-body images of 150 patients: for bone tumors, there are 12 patients with a normal BMI, 17 with overweight, and 21 with obesity. 17, 15, and 18 patients with a normal BMI, overweight, and obesity for liver tumor. While for lung tumors there are 18 patients with a normal BMI, 17 with overweight, and 15 with obesity. The doses injected of 18F-FDG are (6.89±2.28, 7.5±1.21, 8.00±0.96) with normal weight, overweight, and obese, respectively. For bone tumors Mean ± SD injected 18F-FDG activity is 7.74±1.73 mCi in patients with normal BMI and 8.91±1.03 mCi in obese patients and 8.1±0.96 with overweight. For liver, the average maximum 18F-FDG uptake of the tested lung for the three BMI categories is presented in Table 6. The uptake of 18F-FDG is generally higher as BMI increases. Subsequently, we conducted comparisons among the three groups, which demonstrated a statistically significant difference among all groups [81-83].

Table 6 Results for administered 18F-FDG.

Groups	Mean ± SD					
	W (kg)	H(m)	BMI $kg/(m)^2$	Injection dose (mCi)	Dose/weight (mci/kg)	p-value
For bone						
Normal weight	68.25± 12.14	1.73±0.13	22.49±2.006	6.89±1.03	0.10±0.012	<0.05
Overweight	71.29±12.17	1.6±0.11	27.56±1.41	7.5±1.21	0.10±0.01	<0.05
Obese	90.66±14.02	1.62±0.1	34.22±4.02	8.00±0.96	0.08±0.01	<0.05
For liver						
Normal weight	62.17±9.05	1.72±0.09	21.08±3.02	7.74±1.73	0.12±0.03	<0.05
Overweight	74.33±9.70	1.64±0.09	27.32±1.88	8.1±0.96	0.10±0.01	<0.05
Obese	95.77±16.74	1.62±0.16	36.36±5.72	8.91±1.03	0.09±0.009	<0.05
For lung						
Normal weight	63.33±10.22	1.68±0.10	22.06±2.03	6.93±0.88	0.11±0.01	<0.05
Overweight	76.11±10.41	1.66±0.1	27.36±1.02	7.42±1.00	0.09±0.01	<0.05
Obese	89.93±11.76	1.61±0.1	34.57±3.13	8.65±1.00	0.09±0.0006	<0.05

The SUVmax of the bone, liver, and lung are shown in Table 7. SUVmax in all tissues are significantly higher in obese patients than in normal patients ($P > 0.001$). For bone, the mean value for SUVmax is (6.70±1.44) and statistically significant with BMI for normal weight ($p < 0.05$), as shown in Table 4.10. The mean values for SUVmax for overweight and obese are (7.16±1.07) and (8.63±1.25), respectively, with also significant ($p < 0.05$). Upon examining the average liver SUVmax values based on BMI, Table 7) the results are observed a significant increase in SUV among obese individuals. For

liver the mean value of BMI SUVmax is (6.90±1.25), (7.78±0.95), (8.56±1.08), for normal weight, overweight, and obese, respectively, the results showed a significant change between SUVmax and BMI, p value < 0.05. Mean ± SD SUVmax, of the lung is shown in table 7. Mean SUVmax in the lung is significantly higher in obese than those in normal BMI. The relationships between the injection dose and BMI and SUVmax are shown in Figure 3 and 4.

Table 7 SUVmax values based on BMI.

Groups	Mean ± SD				
	Weight (kg)	Height (m)	BMI kg/(m)^2	SUV_{max}(g/ml)	p-value
For bone					
Normal weight	68.25± 12.14	1.73±0.13	22.49±2.006	6.70±1.44	<0.05
Overweight	71.29±12.17	1.6±0.11	27.56±1.41	7.16±1.07	<0.05
Obese	90.66±14.02	1.62±0.1	34.22±4.02	8.63±1.25	<0.05
For liver					
Normal weight	62.17±9.05	1.72±0.09	21.08±3.02	6.90±1.25	<0.05
Overweight	74.33±9.70	1.64±0.09	27.32±1.88	7.78±0.95	<0.05
Obese	95.77±16.74	1.62±0.16	36.36±5.72	8.56±1.08	<0.05
For lung					
Normal weight	63.33±10.22	1.68±0.10	22.06±2.03	6.58±0.72	<0.05
Overweight	76.11±10.41	1.66±0.1	27.36±1.02	7.77±0.87	<0.05
Obese	89.93±11.76	1.61±0.1	34.57±3.13	8.69±1.00	<0.05

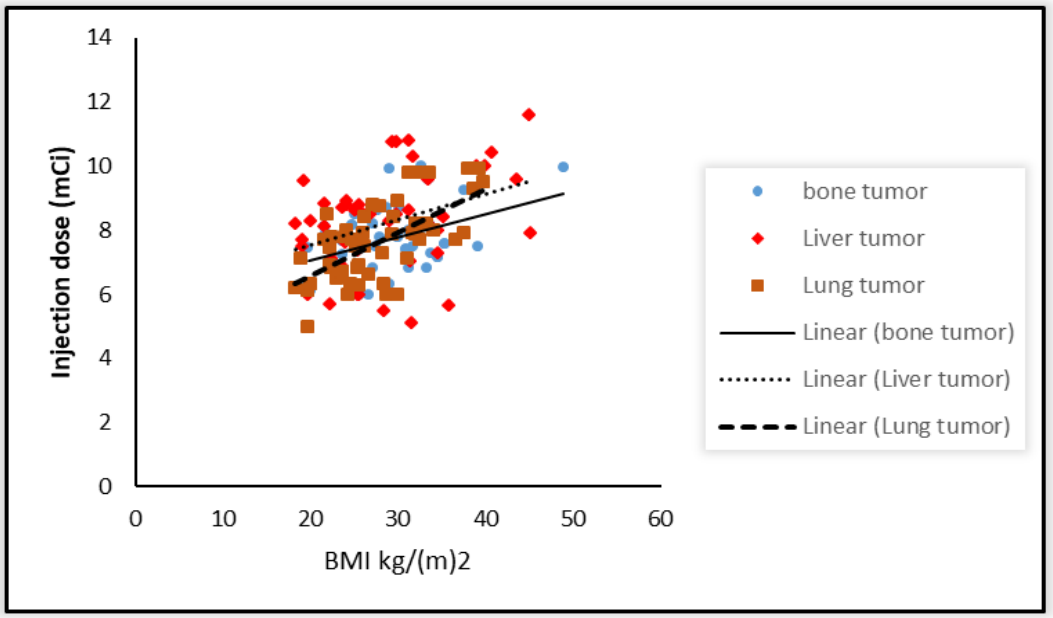

Figure 3 Relation between BMI and 18F-FDG for tumor tissue.

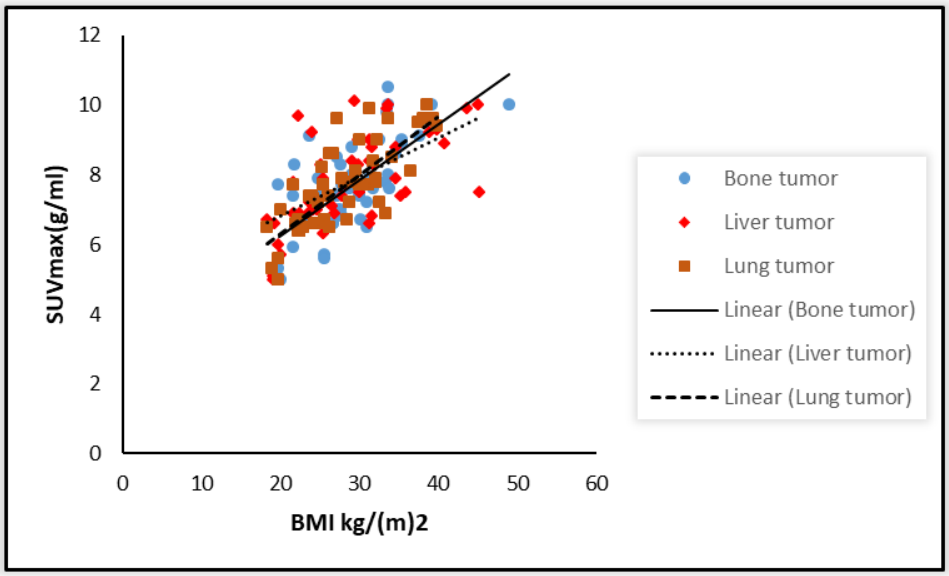

Figure 4 Relation between BMI and SUVmax for tumor tissue.

The SUV (Standardized Uptake Value) is a PET metric that is frequently employed to assess the uptake of various radiopharmaceuticals in both normal tissues and lesions. Multiple studies have indicated that the quantitative evaluation of 18F-FDG absorption is advantageous for distinguishing between malignant and benign tumors and determining the effectiveness of therapies in carcinoma patients [15, 16]. The 18F-FDG-PET images must be accurately interpreted in order to facilitate this separation. The interpreter must possess a comprehensive understanding of the standardized uptake values (SUVs) of healthy organs and the physiological absorption of 18F-FDG. After injecting FDG into the bloodstream, the brain receives approximately 6.9% of the administered dose, the liver receives 4.4%, the heart receives 3.3%, the bone marrow receives 1.7%, the kidneys receive 1.3%, and the lungs receive 0.9%. Different parts of the body have different amounts of 18F-FDG, which shows that its physiological uptake and SUV values are also different [17]. The SUV is a reliable method for determining the level of radiopharmaceutical uptake in both lesions and normal tissues. However, it can be influenced by patient/biological and technical factors, which may lead to either overestimation or underestimating of the activity in lesions and tissues. Factors that can affect the quality of medical imaging include inadequate patient preparation, elevated blood glucose and insulin levels, the patient's diabetic status, body mass index (BMI) or amount of body fat, age, gender, the time between radiotracer injection and imaging start, significant leakage of activity, parameters used for image acquisition and reconstruction, conditions during the period after injection, incorrect entry of patient data such as weight, height, and injected activity into the computer, the impact of CT contrast material on PET images that have been corrected for attenuation, patient and organ movements, and the influence of other diseases and medications on the uptake of 18F-FDG, among others [18-21]. Overweight individuals frequently overestimate SUV in both tumors and normal tissues [22]. SUV gives a more exact assessment of radiopharmaceutical uptake, allowing for more accurate comparisons between PET examinations. Zasadny et al. The study revealed that the SUVs of blood, liver, and spleen are up to double those of persons with lighter body weight [23]. In our investigation, SUVs in bone, lung, and liver are significantly higher in obese patients than in those with a normal BMI (Table 4, and 7). According to Table 4,7, liver uptake has a significant and somewhat positive correlation with BMI. Similar to our findings, Malladiet al. [24], Kamimura et al. [25], and Mahmud et al. [26] discovered a strong correlation between BMI and hepatic 18F-FDG absorption. People with a higher body mass index (BMI) have more fatty tissues, which don't take in much glucose when they're

fasting. This means that more of the 18F-FDG that is injected can still be absorbed by other organs, like the liver [27]. Büsing et al. observed, however, that a high BMI reduced the mean SUVmax in a number of healthy organs, including the liver [28]. There have been prior reports on the effects of body weight and BMI on tissue FDG delivery [29]. The normal tissue FDG uptake is higher in individuals with higher BMIs than in patients with lower BMIs, according to our research. This is probably because non-fatty tissue absorbs more FDG during a fast than fat does, as seen in Table 3 and 6. Multiple factors can affect SUVmax, a diagnostic tool for pulmonary conditions. Research has indicated that respiratory motions can potentially lead to an underestimation of pulmonary SUV. [30]. Researchers have explored various approaches to address the issue of respiratory motion, including the use of respiratory gating technology, CT protocol-based methods, and breathing instructions. [31-32]. Nevertheless, in order to reduce the influence of respiratory motion on SUV, we advised the patients to practice controlled and calm breathing to limit any movement caused by respiration.

4. CONCLUSIONS

The metabolic activity of all patients is overestimated by SUV (calculated or normalized by weight); however, the effect is more pronounced in obese patients than in those with a normal BMI. In summary, the absorption of FDG in the liver, lung, and bone is substantially predicted by blood glucose levels and body mass index. BMI is the most significant factor.

References

[1] Y. Wang, R. Barmin, F. M. Mottaghy, F. Kiessling, T. Lammers, R. M. Pallares, Journal of Controlled Release 383 (2005) 113815 https://doi.org/10.1016/j.jconrel.2025.113815
[2] R. M. Pallares, F. Mottaghy, V. Schulz, F. Kiessling, and T. Lammers, The Journal of Nuclear Medicine 63 (2022) 1802 https://doi.org/10.2967/jnumed.122.263895
[3] M. R. Hasan, S. M. Kadam, S. I. Essa, Iraqi Journal of Science 11 (2022) 35 https://doi.org/10.24996/ijs.2022.63.5.15
[4] A. B. Hade, S. I. Essa, East European Journal of Physics 1 (2023) 241 https://doi.org/10.26565/2312-4334-2023-1-32
[5] A. B. Hade, S. M. Kadam, S. I. Essa, East European journal of physics 2 (2023) 277 https://doi.org/10.26565/2312-4334-2023-2-31
[6] A. B. Hade, S. I. Essa, Iraqi Journal of Science (2024) 4704 https://doi.org/10.24996/ijs.2024.65.8(si).2
[7] S. M. Kadam, M. M. Abbas, S. O. Issa, International Journal of Radiation Research 22 (2024) 831 https://doi.org/10.61186/ijrr.22.4.831
[8] M. S. Riyadh, S. O. Issa, Iraqi Journal of Physics 23 (2025) 13 https://doi.org/10.30723/ijp.v23i2.1327
[9] Z. Kadhum, S. O. Issa, Iraqi Journal of Physics 23 (2025) 31 https://doi.org/10.30723/ijp.v23i1.1316
[10] R. Boellaard et al., European Journal of Nuclear Medicine and Molecular Imaging 42 (2014) 328 https://doi.org/10.1007/s00259-014-2961-x
[11] S. Zincirkeser, E. Sahin, M. Halac, and S. Sager, The Journal of International Medical Research 35 (2007) 231 https://doi.org/10.1177/147323000703500207
[12] K. R. Zasadny, R. L. Wahl, Radiology 189 (1993) 847 https://doi.org/10.1148/radiology.189.3.8234714
[13] N. Avril et al., Journal of Clinical Oncology 14 (1996) 1848 https://doi.org/10.1200/jco.1996.14.6.1848
[14] Lowe VJ, Fletcher JW, Gobar L, Lawson M, Kirchner P, Valk P, et al: J Clin Oncol 16 (1998) 1075 10.1200/JCO.1998.16.3.1075

[15] S. YASUDA, H. FUJII, W. TAKAHASHI, S. TAKAGI, M. IDE, and A. SHOHTSU, Clinical Nuclear Medicine 23 (1998) 767 https://doi.org/10.1097/00003072-199811000-00010
[16] R. Boellaard, Journal of Nuclear Medicine 50 (2009) 11S20S https://doi.org/10.2967/jnumed.108.057182
[17] I. Sarikaya, A. Sarikaya, and P. Sharma, Journal of Nuclear Medicine Technology 47 (2019) 313 https://doi.org/10.2967/jnmt.119.226969
[18] N. J. Hoetjes et al., European Journal of Nuclear Medicine and Molecular Imaging 37 (1687) 1679 https://doi.org/10.1007/s00259-010-1462-6
[19] M. Soret, S. L. Bacharach, and I. Buvat, Journal of Nuclear Medicine: Official Publication, Society of Nuclear Medicine 48 (2007) 932 https://doi.org/10.2967/jnumed.106.035774
[20] K. R. Zasadny and R. L. Wahl, Radiology 189 (1993) 847 https://doi.org/10.1148/radiology.189.3.8234714
[21] A. Malladi, M. Viner, T. Jackson, G. Mercier, and R. M. Subramaniam, Journal of Medical Imaging and Radiation Oncology 57 (2012) 169 https://doi.org/10.1111/1754-9485.12015
[22] K. Kamimura et al., Annals of Nuclear Medicine 24 (2010) 157 https://doi.org/10.1007/s12149-009-0338-1
[23] Mahmud MH, Nordin AJ, Saad FFA, Azman AZF, Quant Imaging Med Surg 5 (2015) 700 10.3978/j.issn.2223-4292.2015.05.02
[24] E. E. Kershaw and J. S. Flier, The Journal of clinical endocrinology and metabolism 89 (2013) 2548 https://doi.org/10.1210/jc.2004-0395
[25] Büsing KA, Schönberg SO, Brade J, Wasser K. Nucl Med Biol 40 (2013) 206 10.1016/j.nucmedbio.2012.10.014
[26] K. Kamimura et al., Annals of Nuclear Medicine 24 (2010) 157 https://doi.org/10.1007/s12149-009-0338-1
[27] Erdi YE, Nehmeh SA, Pan T, et al. J Nucl Med. (45) 2004 1287 https://doi.org/10.1118/1.1997467
[28] S. A. Nehmeh et al., Medical Physics 29 (2002) 366 https://doi.org/10.1118/1.1448824
[29] Huang TC, Mok GS, Wang SJ, et al. Phys Med Biol. 56 (2011) 2559 https://doi.org/10.1007/s11671-009-9432-5
[30] I. Alshalal, H. M. I. Al-Zuhairi, A. A. Abtan, M. Rasheed, M. K. Asmail. J. Mech. Behav. Mater. 32 (2023) 1 https://doi.org/10.1515/jmbm-2022-0280
[31] M. Sellam, M. Rasheed, S. Azizi, T. Saidani. Ceram. Int. 50 (2024) 20917 https://doi.org/10.1016/j.ceramint.2024.03.094
[32] O. Alabdali, S. Shihab, M. Rasheed, T. Rashid. 3rd inter. Scient. conf. alkafeel univ. (ISCKU 2021) (2022) https://doi.org/10.1063/5.0066860
[33] M. Rasheed, O. Alabdali, S. Shihab, A. Rashid, T. Rashid, J. Phys.: Conf. Ser. 1999 (2021) 012078 https://doi.org/10.1088/1742-6596/1999/1/012078
[34] N. Assoudi et al. Opt. Quant. Electron. 54 (2022) 9 https://doi.org/10.1007/s11082-022-03927-x
[35] R. Jalal, S. Shihab, M.A. Alhadi, M. Rasheed, J. Phys.: Conf. Ser. 1660 (2020) 012090 https://doi.org/10.1088/1742-6596/1660/1/012090
[36] S. Shihab, M. Rasheed, O. Alabdali, A.A. Abdulrahman, J. Phys.: Conf. Ser. 1879 (2021) 022120. https://doi.org/10.1088/1742-6596/1879/2/022120
[37] A. Keziz, M. Heraiz, M. RASHEED, A. Oueslati. Mater Chem. Phys. 325 (2024) 129757 https://doi.org/10.1016/j.matchemphys.2024.129757
[38] D. Kherifi, A. Keziz, M. Rasheed, A. Oueslati. Ceram. Int. 50 (2024) 30175 https://doi.org/10.1016/j.ceramint.2024.05.317
[39] A. Jaber, M. Ismael, T. Rashid, M. A. Sarhan, M. Rasheed, I. M. Sala. Eureka: Phys. Eng. 4 (2023) 29 https://doi.org/10.21303/2461-4262.2023.002770

[40] T. Rashid, M. M. Mokji, M. Rasheed. J. Optics 36 (2024) 99 https://doi.org/10.1007/s12596-024-02080-w
[41] H. K. Aity, E. Dhahri, M. Rasheed. Ceram. Int. 50 (2024) 54666 https://doi.org/10.1016/j.ceramint.2024.10.324
[42] M. Rasheed, S. Shihab, O. Alabdali, A. Rashid, T. Rashid, J. Phys.: Conf. Ser. 1999 (2021) 012077 https://doi.org/10.1088/1742-6596/1999/1/012077
[43] M. Rasheed, M. Nuhad Al-Darraji, S. Shihab, A. Rashid, T. Rashid. J. Phys.: Conf. Ser. 1963 (2021) 012058 https://doi.org/10.1088/1742-6596/1963/1/012058
[44] A. Keziz, M. Heraiz, F. Sahnoune, M. Rasheed, Ceram. Int. 49 (2023) 32989 https://doi.org/10.1016/j.ceramint.2023.07.275
[45] E. Kadri, K. Dhahri, R. Barillé, M. Rasheed. Phase Transi. 94 (2021) 65 https://doi.org/10.1080/01411594.2020.1832224
[46] D. Bouras, M. Rasheed, Opt. Quantum Electron. 54 (2022) 12 https://doi.org/10.1007/s11082-022-04161-1
[47] A. Zubaidi, L.M. Asaad, I. Alshalal, M. Rasheed, J. Mech. Behav. Mater. 32 (2023) 1 https://doi.org/10.1515/jmbm-2022-0302
[48] M. Rasheed et al., J. Phys.: Conf. Ser. 1999 (2021) 012080 https://doi.org/10.1088/1742-6596/1999/1/012080
[49] M. Rasheed, M.N. Al-Darraji, S. Shihab, A. Rashid, T. Rashid, J. Phys.: Conf. Ser. 1963 (2021) 012059 https://doi.org/10.1088/1742-6596/1963/1/012059
[50] M. Enneffatia, M. Rasheed, B. Louati, K. Guidara, S. Shihab, R. Barillé, J. Phys.: Conf. Ser. 1795 (2021) 012050 https://doi.org/10.1088/1742-6596/1795/1/012050
[51] M. Rasheed, O.Y. Mohammed, S. Shihab, A. Al-Adili, J. Phys.: Conf. Ser. 1795 (2021) 012043 https://doi.org/10.1088/1742-6596/1795/1/012043
[52] A.H. Ali, A.S. Jaber, M.T. Yaseen, M. Rasheed, O. Bazighifan, T.A. Nofal, Complexity 2022 (2022) 1 https://doi.org/10.1155/2022/9367638
[53] M. Rasheed, et al., J. Adv. Biotechnol. Exp. Ther. 6 (2023) 495 https://doi.org/10.5455/jabet.2023.d144
[54] M. Rasheed, I. Alshalal, A.A. Ashed, M.A. Sarhan, A.S. Jaber, Indones. J. Electr. Eng. Comput. Sci. 33 (2024) 653 https://doi.org/10.11591/ijeecs.v33.i1.pp653-660
[55] I.M. Mohammed, M. Rasheed, AIP Conf. Proc. 3321 (2025) 020026 https://doi.org/10.1063/5.0289719
[56] F. Boudou, A. Belakredar, A. Berkane, M. Rasheed. Not. Sci. Biol. 17 (2025) 12183 https://doi.org/10.55779/nsb17212183
[57] F. Boudou, et al., Not. Sci. Biol. 17(3) (2025) 12593. https://doi.org/10.55779/nsb17312593
[58] F. Boudou, A. Guendouzi, A. Belkredar. M. Rasheed, Not. Sci. Biol. 16 (2024) 13837 https://doi.org/10.55779/nsb16211837
[59] R.S. Mahmood et al. J. Mech. Behav. Mater. 34 (2025) 1 https://doi.org/10.1515/jmbm-2025-0040
[60] T. Rashid, M.M. Mokji, M. Rasheed, J. Mech. Behav. Mater. 34 (2025) 77 https://doi.org/10.1515/jmbm-2025-0074
[61] M. Rasheed, M. N. Mohammedali, F. A. Sadiq, M. A. Sarhan, T. Saidani. J. Optics (New Delhi. Print) 54 (2024) 3490 https://doi.org/10.1007/s12596-024-01928-5
[62] A.J. Hussein, M.N. Al-Darraji, M. Rasheed, M.A. Sarhan, IOP Conf. Ser.: Earth Environ. Sci. 1262 (2023) 022007 https://doi.org/ 10.1088/1755-1315/1262/2/022007
[63] A.J. Hussein, M.N. Al-Darraji, M. Rasheed, M.A. Sarhan, IOP Conf. Ser.: Earth Environ. Sci. 1262 (2023) 022005 https://doi.org/10.1088/1755-1315/1262/2/022005
[64] T. Saidani, M. Rasheed, I. Alshalal, A.A. Rashed, M.A. Sarhan, R. Barillé, Res. Eng. Struct. Mater. 10 (2024) 743 http://dx.doi.org/10.17515/resm2023.21ma0922rs

[65] M. A. Sarhan, S. Shihab, B. E. Kashem, M. Rasheed, J. Phy.: Conf. Ser., 1879 (2021) 022122b https://doi.org/10.1088/1742-6596/1879/2/022122
[66] M. Rasheed, O. Alabdali, S. Shihab, J. Phy.: Conf. Ser. 1879 (2021) 032120 https://doi.org/10.1088/1742-6596/1879/3/032120
[67] M. Rasheed, R. Barillé, J. Non-Cryst. Solids., 476 (2017) 1 https://doi.org/10.1016/j.jnoncrysol.2017.04.027.
[68] M. Rasheed, R. Barillé, Opt. Quantum Electron. 49 (2017) 33 https://doi.org/10.1007/s11082-017-1030-7
[69] F. Dkhilalli, S. M. Borchani, M. Rasheed, R. Barille, K. Guidara, M. Megdiche, J. Mater. Sci. Mater. Electron, 29 (2018) 6297 https://doi.org/10.1007/s10854-018-8609-z.
[70] A. Boumezoued, K. Guergouri, Régis Barillé, Rechem Djamil, Mourad Zaabat, M. Rasheed, J. Alloys Compd. 791 (2019) 550 https://doi.org/10.1016/j.jallcom.2019.03.251
[71] N. Ben Azaza et al., Opt. Mater., 96 (2019) 109328 https://doi.org/10.1016/j.optmat.2019.109328
[72] Areej Adnan Hateef, Essebti Dhahri, M. Rasheed, Habiba Kadhim, Z. Abbas, N. Hassan, Physics and Chemistry of Solid State, 25 (2024) 801 https://doi.org/10.15330/pcss.25.4.801-810
[73] M. Rasheed, SuhaShihab, O. Alabdali, H. H. Hassan, J. Phys. Conf. Ser., 1879 (2021) 032113 https://doi.org/10.1088/1742-6596/1879/3/032113
[74] H. K. Aity, M. Rasheed, E. Dhahri, A. A. Hateef, T. Saidani, Journal of Materials Science, 61 (2026) 6226 https://doi.org/10.1007/s10853-026-12241-w
[75] T. Saidani, S. Mokhtari, M. Rasheed, H. Lahmar, M. Trari, Journal of the Indian Chemical Society, 103 (2026) 102499 https://doi.org/10.1016/j.jics.2026.102499
[76] M. RASHEED, A. Khaleefah, Materials Chemistry and Physics, 353 (2026) 132112 https://doi.org/10.1016/j.matchemphys.2026.132112
[77] S. S. Batros, M. Rasheed, H. K. Aity, A. A. Hatef, T. Saidani, Materials Chemistry and Physics, 355 (2026) 132243 https://doi.org/10.1016/j.matchemphys.2026.132243
[78] A. Raghdi, M. Heraiz, M. Rasheed, A. Keziz, Journal of the Indian Chemical Society, 101 (2024) 101413 https://doi.org/10.1016/j.jics.2024.101413
[79] A. I. A. Ali, M. RASHEED, Experimental and Theoretical NANOTECHNOLOGY, 10 (2026) 277 https://doi.org/10.56053/10.s.277
[80] A. Khaleefah, M. RASHEED, Experimental and Theoretical NANOTECHNOLOGY, 10 (2026) 289 https://doi.org/10.56053/10.s.289
[81] Z. S. Ahmed, M. RASHEED, H. S. Ahmed, Experimental and Theoretical NANOTECHNOLOGY, 10 (2026) 329 https://doi.org/10.56053/10.s.329
[82] Z. S. Ahmed, M. RASHEED, H. S. Ahmed, Experimental and Theoretical NANOTECHNOLOGY, 10 (2026) 343 https://doi.org/10.56053/10.s.343
[83] A. I. A. Ali, M. RASHEED, Experimental and Theoretical NANOTECHNOLOGY, 10 (2026) 239 https://doi.org/10.56053/10.s.239